Langmuir
Article
pubs.acs.org/Langmuir

Hierarchically Ordered Microstructures Self-Assembled from Comb−Coil Block Copolymers

Liquan Wang, Jiaping Lin,* and Liangshun Zhang

Key Laboratory for Ultrafine Materials of the Ministry of Education, School of Materials Science and Engineering, East China University of Science and Technology, Shanghai 200237, China

Received November 26, 2008. Revised Manuscript Received January 30, 2009

Using the real-space implemented self-consistent field theory, we undertook an investigation on the hierarchical self-assembly behaviors of comb−coil block copolymers. The comb−coil block copolymers can self-assemble into hierarchical microstructures with two different length scales. Various structure-within-structure morphologies, such as parallel and perpendicular lamella-within-lamella, cylinder-within-lamella, lamella-within-cylinder, and cylinder-within-cylinder, were observed. In the hierarchical structures, the large-length-scale structures are produced by segregation between the coil blocks and comb blocks, and the small-length-scale structures are formed by microphase separation within the comb blocks. Effects of interaction strength and coil block length on the hierarchical phase behaviors were studied, and the phase diagram was mapped out accordingly. Furthermore, the large-length-scale lamellar period as a function of interaction strength was examined. It was found the lamellar periods are greatly dependent on interaction strengths.

Introduction

Hierarchical characteristics of material are ubiquitous in nature.[1−6] Materials having hierarchical structures are widely found in collagen, abalone nacre, and dendrons. The construction of materials presenting complex hierarchical structures such as those observed in natural materials are of great interest because of their promising applications in smart coatings, biosensors, and fuel cells.[7] The self-assembly of soft matter is considered to be an effective approach for constructing microstructure with hierarchical order.[8−13]

Block copolymers composed of two or more chemically different species constitute an important class of soft materials capable of self-assembling into hierarchical microstructures.[14−28] ten Brinke and co-workers reported a hierarchically ordered structure self-assembled from the comb-shaped supramolecules, where the lower-molecular-weight compounds are weakly connected to one block of a block copolymer by intermolecular interactions.[20−26] The structures were reported to have two different kinds of periodicity: the large-length-scale period corresponds to the length of different blocks in the polymeric backbone, and the small-length-scale period is determined by the length of the bound low-molecular-weight compound within the comb blocks. Furthermore, the hierarchical structures with double periodicity were also observed in linear multiblock copolymers composed of one or two end blocks that are significantly

*Corresponding author. Tel: +86-21-64253370. Fax: +86-21-64253539. E-mail: jplinlab@online.sh.cn.

(1) Sanchez, C.; Arribart, H.; Guille, M. M. G. *Nat. Mater.* **2005**, *4*, 277.
(2) Lakes, R. *Nature* **1993**, *361*, 511.
(3) Heuer, A. H.; Fink, D. J.; Laraia, V. J.; Arias, J. L.; Calvert, P. D.; Kendall, K.; Messing, G. L.; Blackwell, J.; Rieke, P. C.; Thompson, D. H.; Wheeler, A. P.; Veis, A.; Caplan, A. I. *Science* **1992**, *255*, 1098.
(4) Tang, Z.; Kotov, N. A.; Magonov, S.; Ozturk, B. *Nat. Mater.* **2003**, *2*, 413.
(5) Zeng, X.; Ungar, G.; Liu, Y.; Percec, V.; Dulcey, A. E.; Hobbs, J. K. *Nature* **2004**, *428*, 157.
(6) Vaia, R.; Baur, J. *Science* **2008**, *319*, 420.
(7) Sanchez, C.; Boissiere, C.; Grosso, D.; Laberty, C.; Nicole, L. *Chem. Mater.* **2008**, *20*, 682.
(8) Ma, X.; Xia, Y.; Chen, E.-Q.; Mi, Y.; Wang, X.; Shi, A.-C. *Langmuir* **2004**, *20*, 9520.
(9) Xu, W.; Lin, H.; Lu, S.; Xi, J.; Wang, Y. *Langmuir* **2008**, *24*, 10895.
(10) Sel, O.; Kuang, D.-B.; Thommes, M.; Smarsly, B. *Langmuir* **2006**, *22*, 2311.
(11) Zhao, Y.; Li, M.; Lu, Q.; Shi, Z. *Langmuir* **2008**, *24*, 12651.
(12) Muthukumar, M.; Ober, C. K.; Thomas, E. L. *Science* **1997**, *277*, 1225.
(13) Tenneti, K. K.; Chen, X. F.; Li, C. Y.; Tu, Y.; Wan, X.; Zhou, Q.-F.; Sics, I.; Hsiao, B. S. *J. Am. Chem. Soc.* **2005**, *127*, 15481.
(14) Matsushita, Y. *Macromelcules* **2007**, *40*, 771.
(15) Tyler, C. A.; Qin, J.; Bates, F. S.; Morse, D. C. *Macromolecules* **2007**, *40*, 4654.
(16) Guo, Z.; Zhang, G.; Qiu, F.; Zhang, H.; Yang, Y.; Shi, A.-C. *Phys. Rev. Lett.* **2008**, *101*, 028301.
(17) Ye, X.; Shi, T.; Lu, Z.; Zhang, C.; Sun, Z.; An, L. *Macromolecules* **2005**, *38*, 8853.
(18) Huang, C. I.; Lin, Y. H. *Macromol. Rapid Commum.* **2007**, *28*, 1634.
(19) Hanski, S.; Houbenov, N.; Ruokolainen, J.; Chondronicola, D.; Iatrou, H.; Hadjichristidis, N.; Ikkala, O. *Biomacromolecules* **2006**, *7*, 3379.
(20) Ikkala, O.; ten Brinke, G. *Science* **2002**, *295*, 2407.
(21) Ruokolainen, J.; Makinen, R.; Torkkeli, M.; Makela, T.; Serimaa, R.; ten Brinke, G.; Ikkala, O. *Science* **1998**, *280*, 557.
(22) Valkama, S.; Kosonen, H.; Ruokolainen, J.; Haatainen, T.; Torkkeli, M.; Serimaa, R.; ten Brinke, G.; Ikkala, O. *Nat. Mater.* **2004**, *3*, 872.
(23) Ruokolainen, J.; ten Brinke, G.; Ikkala, O. *Adv. Mater.* **1999**, *11*, 777.
(24) Ruotsalainen, T.; Turku, J.; Heikkila, P.; Ruokolainen, J.; Nykanen, A.; Laitinen, T.; Torkkeli, M.; Serimaa, R.; ten Brinke, G.; Harlin, A; Ikkala, O. *Adv. Mater.* **2005**, *17*, 1048.
(25) Ikkala, O.; ten Brinke, G. *Chem. Commun.* **2004**, 2131.
(26) Valkama, S.; Ruotsalainen, T.; Nykanen, A.; Laiho, A.; Kosonen, H.; ten Brinke, G.; Ikkala, O.; Ruokolainen, J. *Macromolecules* **2006**, *39*, 9327.
(27) Chen, H.-L.; Lu, J.-S.; Yu, C.-H.; Yeh, C.-L.; Jeng, U-S.; Chen, W.-C. *Macromolecules* **2007**, *40*, 3271.
(28) Matsushita, Y. *Polym. J.* **2008**, *40*, 177.

longer than the other blocks.[29−34] For example, lamellar-within-lamellar structures were found for the undecablock copolymers of PS-*b*-(PI-*b*-(PS-*b*-PI)$_4$)-*b*-PS architecture with two long polystyrene (PS) blocks and a middle multiblock consisting of alternating short polystyrene (PS) and polyisoprene (PI) blocks.[30] The above systems exhibit an unconventional chain connectivity of molecular architectures, where two intrinsic length scales are introduced. This type of molecular design provides a variety of peculiar hierarchical morphologies. These intriguing morphologies greatly inspire intellectual curiosity and motivate our interest in such systems. Encouraged by experimental observations, we present a theoretical study of the structural organization in a type of block copolymer (i.e., the binary comb−coil block copolymer). The comb−coil block copolymer is a simplification of the comb-shaped supramolecular architecture,[20−26] as described above. Shown in Figure 1 is the architecture of the comb−coil block copolymer in which the branches are asymmetrically attached to the homopolymer backbone.

For the comb−coil block copolymers, the stability of ordered phases has been examined within the framework of weak segregation theory.[35,36] It was speculated that depending on system parameters such as the branch number and the volume fraction of coil blocks, two-length-scale microphase separations may take place. The coil blocks are phase separated from the comb blocks; subsequently, a small-length-scale phase separation occurs within the comb blocks. In addition, Yang et al. experimentally studied the PS-*b*-(PS-*g*-PI) comb−coil block copolymers in a selective solvent.[37] The behaviors involving separation between coil blocks and comb blocks were found, which also provide evidence that the comb−coil block copolymers are prone to self-assemble at different length scales. Therefore, the comb−coil block copolymers are expected to produce hierarchical structures, although there have been no hierarchical structures reported in this system to date.

The self-consistent field theory (SCFT) has emerged as a powerful tool for exploring the thermodynamics of inhomogeneous fluids.[38−50] Matsen and Schick developed

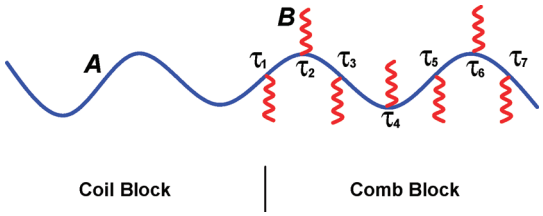

Figure 1. Schematic presentation of the comb−coil block copolymer. Flexible homopolymer B branches are spaced along the flexible homopolymer A blocks. The *j*th branch is located at $\tau_j = \tau_1 + (j-1)(1-\tau_1)/7$. The A blocks between τ_0 and τ_1 are referred to as coil blocks, and the remaining part is referred to as a comb block consisting of B branches and A blocks.

a state-of-the-art numerical approach to solve the SCFT equations.[38−40] The Matsen−Schick spectral approach is suited to accurate calculations of free energies and phase diagrams. To improve the numerical efficiency, in most calculations, the symmetry of the ordered phases is assumed to be known a priori. In addition, the generalization of the spectral method can be used to discover new phases.[16] An alternative numerical approach to solving the SCFT equations was implemented in real space.[42−46] Usually, low-free-energy morphologies are found through relaxation from random potential fields. By giving the initial field possessing symmetry of the order phases, the real-space SCFT can also be utilized to calculate the free energy accurately and construct phase diagrams.[43,44] It was found that the real-space method is preferable over the spectral method because of the large number of basis functions required to obtain an accurate solution for strongly segregated systems in the spectral method. But using a general 3D real-space approach is not beneficial because larger chain contour step numbers for discretization of the diffusion equation are needed at a higher degree of segregation by adopting the Crank−Nicolson algorithm or Baker−Hausdorff operator splitting formula. Recently, the fourth-order backward differentiation formula (BDF4) developed by Fredrickson et al. was utilized to solve the stiff equation for strongly segregated systems.[44,50] This BDF4 method can dramatically decrease the number of contour steps to achieve accurate solutions. Therefore, the real-space SCFT obtained by adopting BDF4 is appropriate to discovering a previous unknown hierarchical structure at a higher degree of segregations in three dimensions.

In this work, we present the first investigation on the hierarchical self-assembly behaviors of comb−coil block copolymers by using real-space SCFT with the BDF4 method. Novel hierarchical microstructures, such as cylinder-within-lamella and cylinder-within-cylinder, were found. Influences of interaction strength and coil block length on the hierarchical phase behaviors were studied. The phase diagram was constructed in space for the interaction strength and coil block volume fraction in the copolymer.

Theoretical Framework

We consider a system with volume V containing n comb−coil block copolymers. As shown in Figure 1, each copolymer is composed of a flexible homopolymer A backbone along which m homopolymer B branches are spaced. The block copolymers are assumed to be monodisperse. The statistical segments of A and B chains are N_A and N_B, respectively. The volume fraction of A-type segment is denoted by f_A, and that

(29) Masuda, J.; Takano, A.; Nagata, Y.; Noro, A.; Matsushita, Y. *Phys. Rev. Lett.* **2006**, *97*, 098301.
(30) Nagata, Y.; Masuda, J.; Noro, A.; Cho, D.; Takano, A.; Matsushita, Y. *Macromolecules* **2005**, *38*, 10220.
(31) Masuda, J.; Takano, A.; Suzuki, J.; Nagata, Y.; Noro, A.; Hayashida, K.; Matsushita, Y. *Macromolecules* **2007**, *40*, 4023.
(32) Nap, R.; Sushko, N.; Erukhimovich, I. Y.; ten Brinke, G. *Macromolecules* **2006**, *39*, 6765.
(33) Subbotin, A.; Klymko, T.; ten Brinke, G. *Macromolecules* **2007**, *40*, 2915.
(34) Klymko, T.; Subbotin, A.; ten Brinke, G. *J. Chem. Phys.* **2008**, *129*, 114902.
(35) Nap, R.; Kok, C.; ten Brinke, G.; Kuchanov, S. I. *Eur. Phys. J. E* **2001**, *4*, 515.
(36) Nap, R.; ten Brinke, G. *Macromolecules* **2002**, *35*, 952.
(37) Xu, F.; Li, T.; Xia, J.; Qiu, F.; Yang, Y. *Polymer* **2007**, *48*, 1428.
(38) Matsen, M. W.; Thompsom, R. B. *J. Chem. Phys.* **1999**, *111*, 7139.
(39) Matsen, M. W.; Schick, M. *Phys. Rev. Lett.* **1994**, *72*, 2660.
(40) Matsen, M. W. *J. Phys.: Condens. Matter* **2002**, *14*, R21.
(41) Jiang, R.; Jin, Q.; Li, B.; Ding, D.; Wickham, R. A.; Shi, A.-C. *Macromolecules* **2008**, *41*, 5457.
(42) Drolet, F.; Fredrickson, G. H. *Phys. Rev. Lett.* **1999**, *83*, 4317.
(43) Fredrickson, G. H. *The Equilibrium Theory of Inhomogeneous Polymers*; Oxford University Press: Oxford, U.K., **2006**.
(44) Cochran, E. W.; Garcia-Cervera, C. J.; Fredrickson, G. H. *Macromolecules* **2006**, *39*, 2449.
(45) Ganesan, V.; Fredrickson, G. H. *Europhys. Lett.* **2001**, *55*, 814.
(46) Drolet, F.; Fredrickson, G. H. *Macromolecules* **2001**, *34*, 5317.
(47) Zhang, L.; Lin, J.; Lin, S. *Macromolecules* **2007**, *40*, 5582.
(48) Zhang, L.; Lin, J.; Lin, S. *J. Phys. Chem B* **2007**, *111*, 351.
(49) Zhang, L.; Lin, J.; Lin, S. *Soft Matter* **2009**, *5*, 173.
(50) Lennon, E. M.; Mohler, G. O.; Ceniceros, H. D.; Garcia-Cervera, C. J.; Fredrickson, G. H. *Multiscale Model. Simul.* **2008**, *6*, 1347.

of B-type segment is $f_B = 1 - f_A$. The jth branch is located at τ_j, given by

$$\tau_j = \tau_1 + \frac{(j-1)(1-\tau_1)}{m} \quad 1 \le j \le m \tag{1}$$

Within the mean-field theory, the configuration of a single copolymer is determined by a set of effective chemical potential fields $\omega_I(\mathbf{r})$ (I = A,B), replacing actual interactions in the melt. The potential fields are conjugated to the density fields $\phi_I(\mathbf{r})$ of block species I. We invoke an incompressibility ($\phi_A(\mathbf{r}) + \phi_B(\mathbf{r}) = 1$) by introducing a Lagrange multiplier $\xi(\mathbf{r})$. For such a system, the free energy (in units of k_BT) per chain is given by

$$F = -\ln\left(\frac{Q}{V}\right) + \frac{1}{V}\int d\mathbf{r}[\chi N\phi_A(\mathbf{r})\,\phi_B(\mathbf{r}) - \omega_A(\mathbf{r})\,\phi_A(\mathbf{r}) - \omega_B(\mathbf{r})\,\phi_B(\mathbf{r}) - \xi(1-\phi_A(\mathbf{r}) - \phi_B(\mathbf{r}))] \tag{2}$$

In this expression, $N(= N_A + mN_B)$ is the total statistical segments of the copolymer, and the Flory−Huggins parameter χ characterizes the interaction between species A and B. $Q = \int d\mathbf{r} q_A(\mathbf{r},1)$ is the partition function of a single noninteracting, branched chain subject to the effective chemical potential fields $\omega_A(\mathbf{r})$ and $\omega_B(\mathbf{r})$ in terms of the backbone propagator $q_A(\mathbf{r}, s)$. The contour length s starts from one end of the homopolymer chain ($s = 0$) to the other ($s = 1$). The spatial coordinate $\mathbf{r}$ is rescaled by R_A, where $R_A^2 = a^2N_A/6$ (a is the statistical segment length). The backbone propagator is divided into $m + 1$ segments based on branch points and is given by

$$q_A(\mathbf{r}, s) = q_A^{(j)}(\mathbf{r}, s) \tag{3}$$

Here, $q_A^{(j)}(\mathbf{r}, s)$ is the backbone propagator for the jth segment between τ_j and τ_{j+1}. In particular, τ_0 and τ_{m+1} are the positions of two free ends of the backbone (i.e., $\tau_0 \equiv 0$ and $\tau_{m+1} \equiv 1$). The contour length s is subject to $\tau_j \le s < \tau_{j+1}$ for $j = 0, 1, ..., m$. Each segment of the backbone propagator satisfies the modified diffusion equation

$$\frac{\partial q_A^{(j)}(\mathbf{r}, s)}{\partial s} = R_A{}^2\nabla^2 q_A^{(j)}(\mathbf{r}, s) - \frac{N_A}{N}\omega_A(\mathbf{r})\, q_A^{(j)}(\mathbf{r}, s) \tag{4}$$

subject to the following initial condition

$$q_A^{(j)}(\mathbf{r}, \tau_j) = q_A^{(j-1)}(\mathbf{r}, \tau_j)\, q_B(\mathbf{r}, 1) \qquad j = 1, 2, ..., m$$

$$q_A^{(0)}(\mathbf{r}, 0) = 1 \tag{5}$$

Here, $q_B(\mathbf{r}, s)$ is a propagator for B branches that satisfies the modified diffusion equation

$$\frac{N_A}{N_B}\frac{\partial q_B(\mathbf{r}, s)}{\partial s} = R_A{}^2\nabla^2 q_B(\mathbf{r}, s) - \frac{N_A}{N}\omega_B(\mathbf{r})\, q_B(\mathbf{r}, s) \tag{6}$$

and is subject to the initial condition $q_B(\mathbf{r}, 0) = 1$ for the free end of the branch at $s = 0$. The backward propagator of the A backbone is similarly subdivided into $m + 1$ segments according to branch points and is given by

$$\overline{q}_A(\mathbf{r}, s) = \overline{q}_A^{(j)}(\mathbf{r}, s) \tag{7}$$

where $\overline{q}_A^{(j)}(\mathbf{r}, s)$ is the backward propagator for the jth segment between $1 - \tau_{m+1-j}$ and $1 - \tau_{m-j}$. The contour length s is subject to $(1 - \tau_{m+1-j}) < s \le (1 - \tau_{m-j})$ for $j = 0, 1, ..., m$. Each segment obeys the diffusion equation (eq 4) and is subject to the following initial conditions:

$$\overline{q}_A^{(j)}(\mathbf{r}, 1-\tau_{m+1-j}) = \overline{q}_A^{(j-1)}(\mathbf{r}, 1-\tau_{m+1-j})\, q_B(\mathbf{r}, 1) \qquad j = 1, 2, ..., m$$

$$\overline{q}_A^{(0)}(\mathbf{r}, 0) = 1 \tag{8}$$

The back-propagator $\overline{q}_{Bj}(\mathbf{r}, s)$ of each B branch attached the jth junction satisfies eq 6 and starts on the end of the B chain tethered to the backbone. The initial condition $\overline{q}_{Bj}(\mathbf{r}, 0)$ is the product of the propagator and backward propagator of the backbone approaching the jth junction and satisfies[51]

$$\overline{q}_{Bj}(\mathbf{r}, 0) = q_A^{(j-1)}(\mathbf{r}, \tau_j)\overline{q}_A^{(m-j)}(\mathbf{r}, 1-\tau_j) = q_A^{j-1}(\mathbf{r}, \tau_j)\overline{q}_A(\mathbf{r}, 1-\tau_j) = \frac{q_A^{(j)}(\mathbf{r}, \tau_j)\overline{q}_A(\mathbf{r}, 1-\tau_j)}{q_B(\mathbf{r}, 1)} = \frac{q_A(\mathbf{r}, \tau_j)\overline{q}_A(\mathbf{r}, 1-\tau_j)}{q_B(\mathbf{r}, 1)} \tag{9}$$

In terms of the single-polymer propagators, the segment densities $\phi_A(\mathbf{r})$ and $\phi_B(\mathbf{r})$ become

$$\phi_A(\mathbf{r}) = \frac{Vf_A}{Q}\sum_{i=1}^{m+1}\int_{\tau_{i-1}}^{\tau_i} ds\, q_A(\mathbf{r}, s)\, \overline{q}_A(\mathbf{r}, 1-s) \tag{10}$$

$$\phi_B(\mathbf{r}) = \frac{Vf_B}{mQ}\sum_{j=1}^{m}\int_0^1 ds\, q_B(\mathbf{r}, s)\, \overline{q}_{Bj}(\mathbf{r}, 1-s) \tag{11}$$

Finally, the minimization of free energy, F, with respect to ϕ_A, ϕ_B, and ξ is achieved by satisfying the mean-field equations

$$\omega_A(\mathbf{r}) = \chi N\phi_B(\mathbf{r}) + \xi(\mathbf{r}) \tag{12}$$

$$\omega_B(\mathbf{r}) = \chi N\phi_A(\mathbf{r}) + \xi(\mathbf{r}) \tag{13}$$

$$\phi_A(\mathbf{r}) + \phi_B(\mathbf{r}) = 1 \tag{14}$$

We decompose the free energy of comb−coil block copolymers (in units of k_BT) as[52]

$$F = E - TS \tag{15}$$

Here, E is the internal energy, and S is the conformational entropy of the total molecule. These quantities are given by

$$E = \frac{\chi N}{V}\int d\mathbf{r}\, \phi_A(\mathbf{r})\, \phi_B(\mathbf{r}) \tag{16}$$

$$-TS = -\ln\left(\frac{Q}{V}\right) - \frac{1}{V}\int d\mathbf{r}[\omega_A(\mathbf{r})\, \phi_A(\mathbf{r}) + \omega_B(\mathbf{r})\, \phi_B(\mathbf{r})] \tag{17}$$

(51) Patel, D. M.; Fredrickson, G. H. *Phys. Rev. E* **2003**, *68*, 051802.
(52) Matsen, M. W.; Bates, F. S. *J. Chem. Phys.* **1997**, *106*, 2436.

To solve the SCFT equations, we use a variant of the algorithm developed by Fredrickson and co-workers.[42−46] The calculations were started from a general initial state. The diffusion equation equations were solved with the fourth-order backward differentiation formula (BDF4), which has higher accuracy and stability for strongly segregated systems.[44,50] For example, the diffusion equation (eq 4) is discretized according to

$$\frac{25}{12}q_{n+1}^{\mathrm{A},j} - 4q_n^{\mathrm{A},j} + 3q_{n-1}^{\mathrm{A},j} - \frac{4}{3}q_{n-2}^{\mathrm{A},j} + \frac{1}{4}q_{n-3}^{\mathrm{A},j} = R_{\mathrm{A}}{}^2\Delta s\nabla^2 q_{n+1}^{\mathrm{A},j} - \Delta s f_{\mathrm{A}}\omega_{\mathrm{A}}(4q_n^{\mathrm{A},j} - 6q_{n-1}^{\mathrm{A},j} + 4q_{n-2}^{\mathrm{A},j} - q_{n-3}^{\mathrm{A},j}) \quad (18)$$

In this expression, $q_{n+i}^{\mathrm{A},j}$ denotes $q_{\mathrm{A}}^{(j)}(\mathbf{r}, s + i\Delta s)$, and Δs is the step size. The initial values required to apply this formula are obtained by using backward Euler and Richardson extrapolation. The densities $\phi_{\mathrm{I}}(\mathbf{r})$ of special I, conjugating the chemical potential fields $\omega_{\mathrm{I}}(\mathbf{r})$, are evaluated with respect to eqs 10−13. The chemical potential fields $\omega_{\mathrm{I}}(\mathbf{r})$ can be updated by using a two-step Anderson mixing scheme.[53]

All of the simulations in this work were carried out in three dimensions with periodic boundary conditions. Each calculation utilized a step size of $\Delta s = 10^{-3}$ along the chain contour for both the A blocks and B branches. After testing several spatial resolutions, we found that the free energy in the system can converge to a stable value when the spatial resolution is smaller than $0.28R_{\mathrm{A}}$.[54] Thus, in the calculations, we chose the spatial resolution $\Delta x < 0.28R_{\mathrm{A}}$. In addition, the adoption of a smaller contour step size can further ensure the accuracy of the calculations.[50] The numerical simulations proceeded until the relative free-energy changes at each iteration were smaller than 10^{-6} and the incompressibility condition was achieved. We minimized the free energy with respect to the size of the simulation box, as suggested by Bonbot-Raviv and Wang.[55] In the simulations, the potential hierarchically ordered micostructures were discovered by the calculations that started from the random initial field. To compare the free energies of different phases, the ordered phase discovered by the simulation started from the random initial field was used as an initial input for the systems under other conditions.[16,43] In these calculations, the simulation box size was also adjusted to minimize the free energy.

Results and Discussion

For the comb−coil block copolymers studied in the present work, the interaction strength χN between A and B blocks is averaged with respect to the number of branches m, as described in our previous work.[48,49,56] Because of the large parameter space of the studied system, such as volume fraction f_{B} of branches, branch number m, the position of the first junction point τ_1, and the average interaction strength $\chi N/m$, we restrict our attention to the comb−coil block copolymers with $f_{\mathrm{B}} = 0.20$ and $m = 7$ for simplicity. The value of m should be large enough to ensure that hierarchical microphase separation occurs,[35,36] but larger m dramatically increases the computational cost, thus a moderate value of $m = 7$ is chosen. For the convenience of presentation, we define the A blocks between τ_0 and τ_1 as coil blocks and the remainder as comb blocks, as shown in Figure 1. Thus, the value of τ_1 is equal to the length of the coil blocks, and the volume fraction of coil blocks can be given by $f_{\mathrm{coil}} = \tau_1(1 - f_{\mathrm{B}})$.

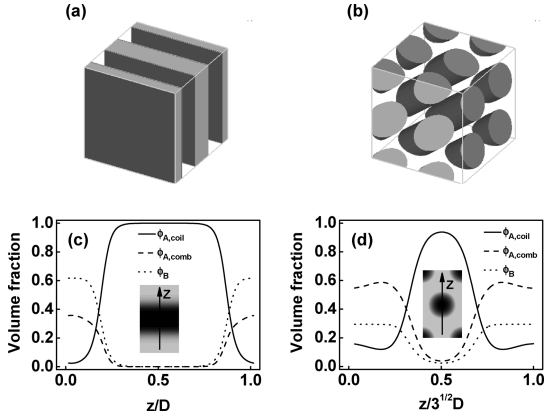

Figure 2. Segment density configuration (light gray corresponds to coil blocks) for comb−coil block copolymers with $f_{\mathrm{B}} = 0.20$, $m = 7$, and $\chi N/m = 15.0$ at different values of τ_1: (a) $\tau_1 = 0.85$ and (b) $\tau_1 = 0.50$. One-dimensional density profiles of coil blocks $\phi_{\mathrm{A,coil}}$, the A backbone of comb blocks $\phi_{\mathrm{A,comb}}$, and branches ϕ_{B}, in different structures are given: (c) lamella, $\tau_1 = 0.85$ and (d) cylinder, $\tau_1 = 0.50$. The spatial coordinate z is expressed in units of D. D is the layer spacing for **L** and the spacing between cylinders for **C**.

We first study the microphase separation behaviors of comb−coil block copolymers close to the order−disorder transition. Lamella (**L**), a cylinder (**C**), a gyriod (**G**), and a sphere (**S**) are formed. For example, the lamellar structure was observed for $\tau_1 = 0.85$ (Figure 2a), and the cylindrical structure was found for $\tau_1 = 0.50$ at $\chi N/m = 15.0$ (Figure 2b). To understand the detailed structure further, we plot the 1D density profiles for the coil blocks, the A blocks of comb blocks, and the branches. As can be seen from 1D density profiles for **L** in Figure 2c and **C** in Figure 2d, the branches and A blocks in comb blocks are mixed homogenously, implying that no phase separation occurs in comb blocks. It is revealed that the phase separations of **L**, **C**, **G**, and **S** structures take place only between the coil blocks and comb blocks. Inverse structures whose minority domains are occupied by comb blocks, such as **S**, **C**, and **G**, are also found. This result is consistent with the weak segregation theoretical predication and experimental observation.[35−37] When the τ_1 value is smaller than about 0.35, a normal spherical structure ($\mathbf{S}_n$) appears, which is not shown in Figure 2. In the $\mathbf{S}_n$ phase, the phase separation takes place between A blocks and B blocks. The comb−coil block copolymers behave as graft copolymers. The phase behaviors of graft coplymers have already been well studied in our previous work.[57]

When the interaction strength between the A and B blocks is increased far above the value of the order−disorder transition, then a hierarchical structure emerges. Figure 3 shows the hierarchical structures obtained for the comb−coil block copolymer system with various values of τ_1 and $\chi N/m$ (the cross sections of the hierarchical structures are also demonstrated for clarity). The light-gray colors are assigned to indicate the B blocks. These structures have two different periods related to the two intrinsic length scales. Taking

(53) Eyert, V. *J. Comput. Phys.* **1996**, *124*, 271.
(54) Heckmann, M.; Drossel, B. *Macromolecules* **2008**, *41*, 7679.
(55) Bohbot-Raviv, Y.; Wang, Z.-G. *Phys. Rev. Lett.* **2000**, *85*, 3428.
(56) Wang, L.; Zhang, L.; Lin, J. *J. Chem. Phys.* **2008**, *129*, 114905.
(57) Zhang, L.; Lin, J.; Lin, S. *J. Phys. Chem. B* **2008**, *112*, 9720.

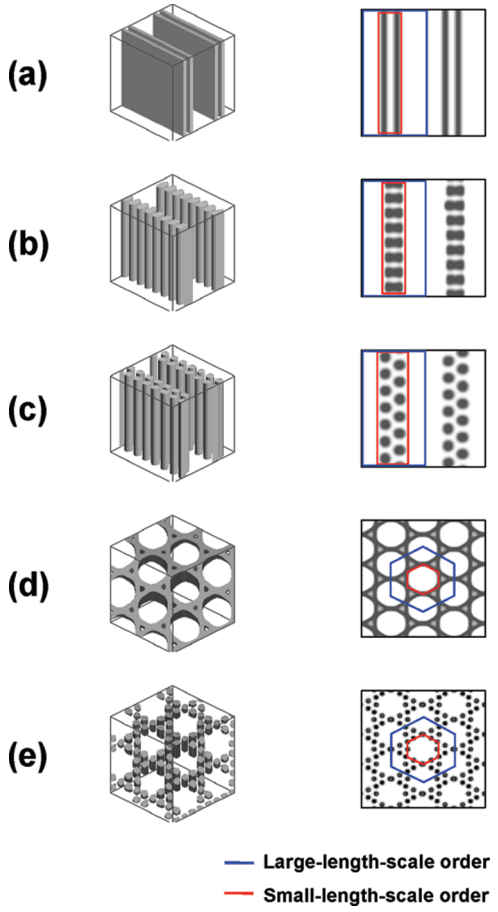

Figure 3. Segment density configuration (left) and cross section (right) (light gray corresponds to B blocks) for comb−coil block copolymers with $f_B = 0.20$ and $m = 7$: (a) parallel lamella-within-lamella, $\tau_1 = 0.85$ and $\chi N/m = 30.0$; (b) perpendicular lamella-within-lamella, $\tau_1 = 0.85$ and $\chi N/m = 50.0$; (c) cylinder-within-lamella, $\tau_1 = 0.70$ and $\chi N/m = 40.0$; (d) lamella-within-cylinder, $\tau_1 = 0.50$ and $\chi N/m = 25.0$; and (e) cylinder-within-cylinder, $\tau_1 = 0.50$ and $\chi N/m = 40.0$. These structures are represented as (small-length-scale structure)-within-(large-length-scale structure). Blue and red rectangles (or hexagons) are used to emphasize the underlying order of large-length-scale and small-length-scale structures, respectively.

Figure 3a as an example, the repeat unit is composed of one thick A lamella and three thin B−A−B lamellae parallel to the thick A lamella. The large-length-scale period corresponds to the thick A lamella and the combined thin lamellae, whereas the small-length-scale period corresponds to the thin lamellae (indicated by the blue and red rectangles, respectively). This structure is referred to as the parallel lamellar-within-lamellar (**L**-in-**L**) structure. In addition, we also define the structures in Figure 3b−e as perpendicular lamella-within-lamella (**L**-in-**L**), cylinder-within-lamella (**C**-in-**L**), lamella-within-cylinder (**L**-in-**C**), and cylinder-within-cylinder (**C**-in-**C**), respectively. These representations are present in the formula as (small-length-scale structure)-within-(large-length-scale structure). For the perpendicular **L**-in-**L** and **C**-in-**L** structures, the thick lamellae are kept in the large-length-order structures, whereas the thin co-alternating lamellae normal to thick lamellae and two-row cylinders are respectively produced in small-length-order structures. For the **L**-in-**C** and **C**-in-**C** structures, the B branches self-assemble into 6 small-length-scale lamellae and 12 small-length-scale cylinders around the large-length-scale A cylinders arranged on a hexagonal lattice, respectively.

To gain more information about the hierarchical ordered structures, the 2D density distributions of various blocks of comb−coil block copolymers are plotted in Figure 4. Five structures are shown: parallel **L**-in-**L** and perpendicular **L**-in-**L**, **C**-in-**L**, **L**-in-**C**, and **C**-in-**C**. Because of the similarity of phase separation in these structures, only the perpendicular **L**-in-**L** and **C**-in-**C** structures are described in detail below. For perpendicular **L**-in-**L** structure in Figure 4b, the coil blocks self-assemble into the thick A domains, and the A and B blocks in comb blocks self-assemble into alternating lamellae that are aligned perpendicular to the thick A domains. For **C**-in-**C**, the coil blocks segregate into the large-length-scale cylinders hexagonally embedded in a matrix formed by comb blocks, as shown in Figure 4e. In the matrix, the B branches produce the small-length-scale cylinders dispersed in the domains rich in A blocks of comb blocks. On the basis of the results, the correponding schematic illustration of these hierarchical structures is shown in Figure 4. The light-red, light-blue, and white regions denote B branch domains, A coil block domains, and domains rich in A blocks of comb blocks, respectively. The possible molecular organizations in these structures are also presented. The blue line and red lines represent A blocks and B blocks, respectively. Regarding all of these structures, the large-length-scale assembly is attributed to phase separation between the coil blocks and comb blocks, and the small-length-scale ordering inside the comb block domains is driven by the segregation between A and B blocks in comb blocks.

Summarizing the simulation results for comb−coil block copolymers with $f_B = 0.20$ and $m = 7$ at various values of average interaction strength and coil block length, we plot the phase diagram in $\chi N/m$−f_{coil} space, where f_{coil} is the volume fraction of coil blocks in the copolymer. The phase diagram is presented in Figure 5. Figure 5a shows the phase diagram at lower value of the interaction strength, where classic phases are formed. The phase boundaries are obtained by comparing the free energies of different structures. In these structures, the minority domains are occupied by the coil block on the left side of the critical point and the comb block on the right side of the critical point. The order−disorder transtion shifts toward higher value of $\chi N/m$ as f_{coil} decreases. With increasing value of the interaction strength, the **S** → **C** → **G** → **L** phase transitions are observed at certain value of f_{coil}. The gyroid strucutures are found to exist in a narrow range of the phase diagram and become unstable when the average interaction strength is larger than about 16.2. The phase diagram is not symmetrical about $f_{coil} = 0.50$. Thus, the comb−coil block copolymers behave rather as the asymmetry block copolymer at weak segregation.

Figure 5b shows the phase diagram at higher value of interaction strength, where hierarchical structures emerge. The phase boundaries are drawn to guide the eye on the basis of the simulation points. Two different lines are included in the diagram. The solid lines are denoted as the occurrence of phase transtions at large length scales. As the f_{coil} value decreases in the diagram from right to left, the sequence of large-length-scale ordered phases is as follows: lamella (including **L**, **L**-in-**L**, and **C**-in-**L**) → cylinder (including **C**, **L**-in-**C**, and **C**-in-**C**) → sphere ($\mathbf{S}_n$). The dashed lines indicate the phase boundaries where phase separation at small length scales occurs. As the average interaction strength $\chi N/m$ increases in the diagram from bottom to top, **L** → (parallel **L**-in-**L**) → (perpendicular **L**-in-**L**), **L** → (parallel **L**-in-**L**) → (**C**-in-**L**), and **C** → (**L**-in-**C**) → (**C**-in-**C**) phase transtions take

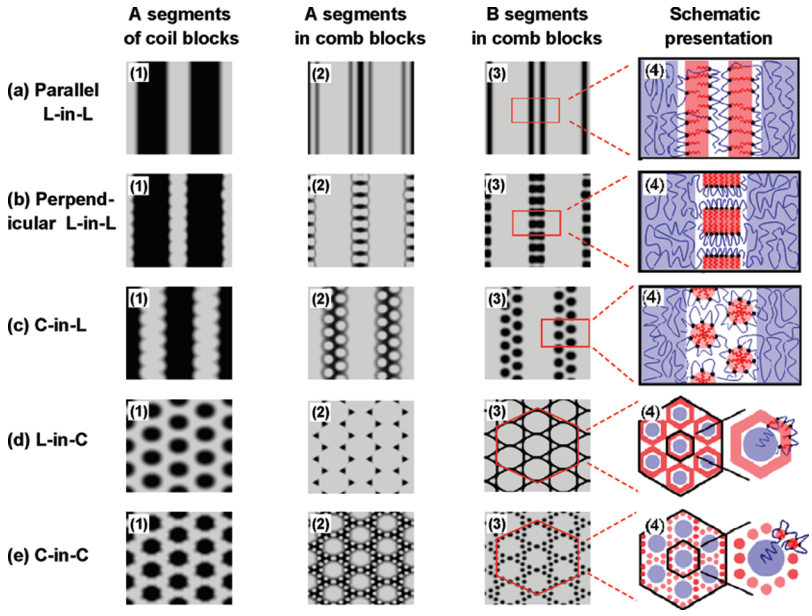

Figure 4. Two-dimensional density plots of (1) coil blocks, (2) A blocks of comb blocks, and (3) branches for various structures: (a) parallel lamella-within-lamella, (b) perpendicular lamella-within-lamella, (c) cylinder-within-lamella, (d) lamella-within-cylinder, and (e) cylinder-within-cylinder. Dark- and light-gray regions indicate high and low local volume fractions of a species, respectively. Image 4 shows corresponding schematic illustrations, where the light-blue, white, and light-red regions represent coil block domains, domains rich in A blocks of the comb block, and branch domains, respectively. The blue and red lines denote the A and B blocks, respectively.

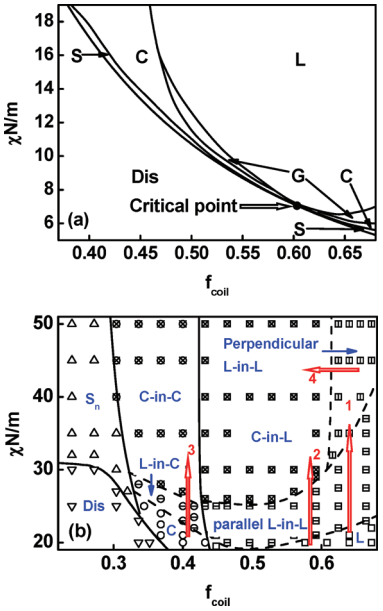

Figure 5. Phase diagram in $\chi N/m$–f_{coil} space for comb–coil block copolymer with $m = 7$ and $f_B = 0.20$ in different segregation regions: (a) weak segregation and (b) higher segregation. Dis labels the regions where the melt is disordered. The ordered regions include **L** (lamella), **C** (cylinder), **G** (gyroid), **S** (sphere), parallel **L**-in-**L** (parallel lamella-within-lamella), perpendicular **L**-in-**L** (perpendicular lamella-within-lamella), **L**-in-**C** (lamella-within-cylinder), **C**-in-**C** (cylinder-within-cylinder), and $\mathbf{S}_n$ (normal sphere). In plot a, the phase boudaries are determined by comparing the free energies of **L**, **C**, **G**, and **S**, whose minority domains are formed by either coil blocks or comb blocks. In plot b, the phase boudaries are drawn to guide the eye on the basis of the calculated points.

place at different f_{coil} values, as respectively traced by arrows 1–3. In these transtions, the structures on the large length scale remain the same while the phase transition on the small length scale takes place. For example, in the **L** → (parallel **L**-in-**L**) → (**C**-in-**L**) phase transtion, the large-length-scale structures remain in the lamellar phase, whereas the small-length-scale structures transform from disordered to lamella and then to cylinder. Furthermore, when the f_{coil} value decreases, there is also a phase transtion from lamella to cylinder on the small length scale, corresponding to the (perpendicular **L**-in-**L**) → (**C**-in-**L**) transtion in the phase diagram, which is traced by arrow 4.

It can be noted from the phase diagram that the parallel **L**-in-**L** survives over a narrow range of $\chi N/m$ in the phase transtions from **L** to perpendicular **L**-in-**L** or **C**-in-**L** with increasing $\chi N/m$ values (arrows 1 and 2 in Figure 5b), indicating that parallel **L**-in-**L** becomes unstable in the strong segregation regimes. The reason that the system assumes the perpendicular **L**-in-**L** or **C**-in-**L** rather than parallel **L**-in-**L** structure at higher values of the interaction strength arises from the interplay of enthalpic and entropic effects. To compare the free energies of perpendicular **L**-in-**L** or **C**-in-**L** with those of parallel **L**-in-**L**, the metastable parallel **L**-in-**L** structure is also calculated, having been obtained by seeding the simulation with the initial field possessing lamellar symmetry.[43] The different free-energy contributions to the perpendicular **L**-in-**L** (**C**-in-**L**) and parallel **L**-in-**L** structures are displayed in Table 1. The total free energy is decomposed into interaction energy E and the contribution of conformational entropy $-TS$. Table 1 shows that the loss of conformational entropy is greater but the interaction energy is lower in the perpendicular **L**-in-**L** (**C**-in-**L**) relative to the corresponding values for parallel **L**-in-**L**. As a result, perpendicular **L**-in-**L** (**C**-in-**L**) exhibits a lower total free energy. When the molecules are organized in the perpendicular **L**-in-**L** (**C**-in-**L**) structure, although the entropic loss is much larger than that in parallel **L**-in-**L**, this is more than compensated for by the fact that the interaction enthalpy can be reduced. Thus, the contribution from the enthalpic interaction plays a dominant role in determining the preferred perpendicular **L**-in-**L** (**C**-in-**L**) structure at higher interaction strength.

Table 1. Comparison of Total Free Energy F, Interaction Energy E, and Contribution of Conformational Entropy $-TS$ for (a) the Parallel and Perpendicular Lamellar-within-Lamellar Structures at $\tau_1 = 0.85$ and $\chi N/m = 50.0$ and (b) the Parallel Lamellar-within-Lamellar and Cylindrical-within-Lamellar Structures at $\tau_1 = 0.70$ and $\chi N/m = 40.0$

(a)	parallel lamella-within-lamella	perpendicular lamella-within-lamella
F	31.753	31.483
E	16.818	14.506
$-TS$	14.945	16.986
(b)	parallel lamella-within-lamella	cylinder-within-lamella
F	33.933	33.227
E	18.126	15.895
$-TS$	15.817	17.332

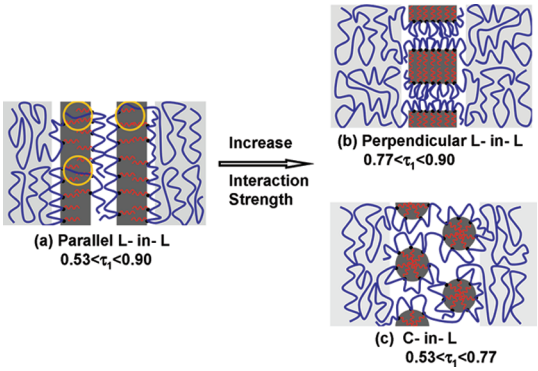

Figure 6. Schematic illustrations of (a) parallel lamella-within-lamella, (b) perpendicular lamella-within-lamella, and (c) cylinder-within-lamella for the comb−coil block copolymer system. The light-gray, white, and dark-gray regions represent coil block domains, domains rich in A blocks of the comb block, and branch domains, respectively. The blue and red lines denote the A and B blocks, respectively.

The fact that the interaction energy in the parallel **L**-in-**L** structure is higher than that in the perpendicular **L**-in-**L** (**C**-in-**L**) structure can be further understood by referring to the cartoon in Figure 6. As indicated in Figure 6a, to produce the small-length-scale A layer in the parallel **L**-in-**L**, the A blocks should form "bridges" (indicated by yellow circles) across the B branch layers as a result of the continuous character of the A chains. The crossing of A blocks on dissimilar B domains dramatically increases the interaction energy between A and B blocks as the interaction strength increases. However, for the perpendicular **L**-in-**L** (**C**-in-**L**) structure, as shown in Figure 6b (Figure 6c), this unfavorable interaction can be avoided. Thus, the interaction enthalpy in parallel **L**-in-**L** is higher than that in perpendicular **L**-in-**L** (**C**-in-**L**). Consequently, the perpendicular **L**-in-**L** (**C**-in-**L**) structure is more energetically favorable at higher $\chi N/m$. The same reason holds for the situation in which the **L**-in-**C** structure becomes unstable at higher $\chi N/m$ (arrow 3 in Figure 5b), where the analogous bridges also appear in **L**-in-**C** as illustrated in Figure 4d.

The phase diagram also demonstrates that the variation of the f_{coil} value or the τ_1 value (τ_1 is related to f_{coil} through $f_{coil} = \tau_1(1 - f_B)$) can induce the (perpendicular **L**-in-**L**) → (**C**-in-**L**) phase transition (arrow 4 in Figure 5b). In this phase transition, the lamella → cylinder transition takes place on a small length scale, whereas the large-length-order structures remain lamellar patterns. The total free energies of **C**-in-**L** and perpendicular **L**-in-**L** plotted against τ_1 is shown in Figure 7. Figure 7 reveals that the perpendicular **L**-in-**L** structure has the lowest free energy when the τ_1 value is larger than 0.77, implying that the (perpendicular **L**-in-**L**) → (**C**-in-**L**) phase transition occurs at $\tau_1 = 0.77$. This phase transition can be ascribed to the symmetry changes of comb blocks. The composition of branches in comb blocks is calculated as a function of τ_1, and it is shown in the bottom panel. At $\tau_1 = 0.77$ where the transition takes place, the composition of branches in comb blocks is about 0.52. Our previous calculations of symmetric graft copolymers indicate that a phase transition from lamella to cylinder occurs when the composition of branches is about 0.52 when interaction strength is strong.[56,57] Thus, we can conclude that the comb−coil block copolymers undergo conventional phase transitions at small length scales, such as those observed in diblock and graft copolymers,[39,56,57] and the phase boundaries of small-length-scale structural transition are mainly determined by the properties of comb blocks.

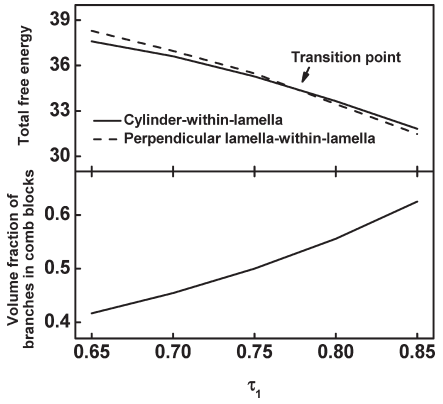

Figure 7. Dependence of the total free energy and branch volume fraction in comb blocks on the position of the first junction for comb−coil block copolymers with $f_B = 0.20$ and $m = 7$ at $\chi N/m = 50.0$. In the up panel, the total free energies for the cylinder-within-lamella (solid curve) and perpendicular lamella-within-lamella (dashed curve) are plotted against the position of the first junction. In the bottom panel, the branch volume fraction in comb blocks is plotted against the position of the first junction.

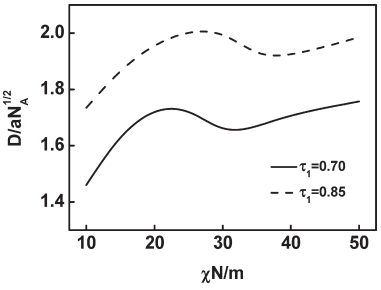

Figure 8. Domain spacing $D/aN_A^{1/2}$ as a function of average interaction strength $\chi N/m$ for lamellar structures of comb−coil block copolymers with $f_B = 0.20$ and $m = 7$ at $\tau_1 = 0.70$ and $\tau_1 = 0.85$, respectively.

The domain size is an important characteristic of ordered structures. For a hierarchically ordered structure, the change in structure at small length scales has a significant effect on the domain period at large length scales. Figure 8 presents the lamellar period as a function of average interaction strength $\chi N/m$. The lamellar period is the period of lamellar

structures at large length scales. The period was plotted for both $\tau_1 = 0.70$ and $\tau_1 = 0.85$. Concomitantly with increasing the interaction strength, the structures develop as follows: **L** → (parallel **L**-in-**L**) → (perpendicular **L**-in-**L**) at $\tau_1 = 0.85$ and **L** → (parallel **L**-in-**L**) → (**C**-in-**L**) at $\tau_1 = 0.70$. For both cases, upon increasing the value of $\chi N/m$, the lamellar period increases monotonically to a local maximum, followed by a decrease to a local minimum, and then increases slowly. When $\chi N/m$ is lower, the comb−coil block copolymers undergo phase separation only between the coil blocks and comb blocks, and the period variation is similar to the situation observed for diblock copolymers.[38] The lamellar period increases as $\chi N/m$ increases. When the secondary domain appears as $\chi N/m$ increases, a reduction in the lamellar period takes place. With further increasing $\chi N/m$, the A and B blocks in the secondary domain become relatively well separated and the lamellar period has a local minimum. Keeping increasing $\chi N/m$, the lamellar period increases as a result of the increasing repulsion between the A and B blocks.[32]

The present comb−coil block copolymer systems, investigated for $f_B = 0.20$ and $m = 7$, exhibit very rich phase behaviors. Various hierarchical structure-within-structure morphologies are observed. Because no experimental studies on hierarchical structures of such comb−coil block copolymer systems are available, it is difficult to make a direct comparison between theoretical predictions and experimental observations. However, there are still some existing experimental phenomena regarding the hierarchical structures in the literature, supporting our theoretical predictions. For example, many two-length-scale hierarchical morphologies were observed in the comb-shaped supramolecular system, such as PS-*b*-P4VP(PDP)$_{1.0}$, where 3-pentadecylphenol (PDP) is hydrogen bonded to pyridine.[20−26,58] In this system, the large-length-scale structures are formed by the phase separation of the coil block (PS) and comb block (P4VP(PDP)$_{1.0}$), whereas the small-length-scale-structures are formed as a result of the self-assembly of the comb block (P4VP(PDP)$_{1.0}$). Upon increasing the volume fraction of coil block (PS) chains, at large length scales the coil block (PS) domains are transformed from spheres to cylinders to lamellae and then eventually become a matrix. However, at small length scales, the structures remain as lamellar patterns. In our calculations, we found a transition from cylinder-within-cylinder to cylinder-within-lamella with increasing coil block length, as shown in Figure 5b. In this transition, the branch blocks form small-length-scale cylinders and remain unchanged, and coil blocks are transformed from cylinder to lamella at large length scales. Such phase behavior (i.e., large-length-scale structures change whereas small-length-scale structures remain unchanged as the coil block length varies) is well in line with experimental observations, although the studied systems are different.

In the present calculations, we found a transition from parallel **L**-in-**L** to perpendicular **L**-in-**L** as the interaction strength increases (indicated by arrow 1 in Figure 5b). In this transition, the thin lamellae parallel to thick lamellae transform to the thin lamellae perpendicular to thick lamellae. Similar transitions from parallel lamellae to perpendicular lamellae were also observed in confined block copolymer thin films.[59,60] The reasons for the phase transitions of both systems come from the balance between enthalpic and entropic effects. In the thin film, although the perpendicular phase has a less favorable surface energy, the entropy can be reduced because its period is free to relax to the bulk spacing.[59] However, in the present system, there is an inverse interplay of enthalpic and entropic effects. When the comb−coil block copolymers transform from parallel **L**-in-**L** to perpendicular **L**-in-**L** structures, although the entropy is increased, the interaction energy is decreased through avoiding the unfavorable bridge across dissimilar domains.

Hierarchical self-assembly is an interesting phenomenon that is widely observed in nature.[1−6] The exploitation of comb−coil block copolymers greatly expands the morphological window of block copolymers. In this work, we presented the first example, to the best of our knowledge, of hierarchically ordered microstructures self-assembled from binary comb−coil block copolymers. Various novel hierarchical microstructures are found. These results gained through SCFT calculations may provide a useful guide for manufacturing highly functional materials with new hierarchical order, which can lead to various applications such as optical devices. The approaches are also helpful for understanding other hierarchical structures, such as sphere-within-lamella, that may exist in block copolymer systems with complicated architectures.

Conclusions

In summary, we applied the SCFT implemented in real space to investigate the hierarchically ordered structures self-assembled from comb−coil block copolymers. The comb−coil block copolymers exhibit hierarchically ordered microstructures, including parallel and perpendicular lamella-within-lamella, cylinder-within-lamella, lamella-within-cylinder, and cylinder-within-cylinder. In these microstructures, the large-length-scale structures are formed by phase separation between the coil blocks and comb blocks, whereas the small-length-scale structures are produced by phase separation between the B branches and A blocks in comb blocks. Both the interaction strength and the first junction position parameters significantly influence the hierarchical self-assembly behaviors. The phase diagram was mapped out to show the relationship between microstructures and these parameters. The large-length-scale lamellar periods as a function of interaction strength at different coil block lengths were also studied. The interaction strength exerts a marked effect on the period of structures.

Acknowledgment. This work was supported by the National Natural Science Foundation of China (50673026 and 20574018). Support from the Doctoral Foundation of Education Ministry of China (grant no. 20050251008) and the Projects of Shanghai Municipality (06SU07002, 082231, and B502) is also appreciated.

(58) Tung, S.-H.; Kalarickal, N. C.; Mays, J. W.; Xu, T. *Macromolecules* **2008**, *41*, 6453.

(59) Matsen, M. W. *J. Chem. Phys.* **1997**, *106*, 7781.

(60) Pickett, G.; Balazs, A. C. *Macromolecules* **1997**, *30*, 3097.